Stable isotopes in precipitation and meteoric water: Sourcing and tracing the North American monsoon in Arizona, New Mexico, and Utah

Crystal Lynn Tulley-Cordova[1,1], Annie L Putman[2,2], and Gabriel Bowen[2,2]

[1]Navajo Nation Department of Water Resources
[2]University of Utah

January 20, 2023

Abstract

The North American monsoon (NAM) is an important source of precipitation across the southwestern United States (US). The approximate northern boundary of this feature crosses the Navajo Nation, in the Four Corners region, where NAM rains have long been important to the livelihoods of Native Americans. Relatively little is known about the characteristics and hydrological significance of the NAM in this region. Here we report a new 4-year record of stable H and O isotope ratios in monsoon-season rainfall and water resources across the Navajo Nation. Monthly precipitation samples collected at 39 sites document a characteristic pattern of ^{2}H- and ^{18}O-enrichment associated with monsoonal precipitation. These changes are weakly correlated with local precipitation intensity, however, and the correlation that does exist is dominated by sub-cloud evaporation effects. In contrast to precipitation amount, monsoon-season isotopic values exhibited limited spatial variability across the region, and after correction for sub-cloud evaporation Navajo Nation values were similar to those from a site in southern Arizona. Airmass back-trajectory analysis suggests that the uniformly high NAM isotope values across the region may reflect 1) a region-wide shift from mid-latitude to low-latitude moisture sources at the onset of the peak monsoon, and 2) substantial land-surface recycling of NAM moisture in upwind regions. Comparison of precipitation isotope data with surface and groundwater values implies that, despite its hydroclimatic significance, monsoon rainfall contributes little to rand subsurface water resources. This highlights the monsoon's importance for warm-season land-surface ecology and hydrology critical to residents of the Four Corners region.

Hosted file

`essoar.10506650.2.docx` available at https://authorea.com/users/555666/articles/606145-stable-isotopes-in-precipitation-and-meteoric-water-sourcing-and-tracing-the-north-american-monsoon-in-arizona-new-mexico-and-utah

Stable isotopes in precipitation and meteoric water: Sourcing and tracing the North American monsoon in Arizona, New Mexico, and Utah

C.L. Tulley-Cordova[1,2], A.L. Putman[2], and G.J. Bowen[2]

[1]Navajo Nation Water Management Branch, Fort Defiance, AZ, USA.

[2]Department of Geology and Geophysics, University of Utah, Salt Lake City, UT, USA.

Corresponding author: Crystal Tulley-Cordova (tulleycordova@gmail.com)

Key Points:

1. A prominent seasonal maximum in Four Corners-region precipitation isotope ratios occurs during the peak of the North American Monsoon
2. Peak monsoon precipitation isotope ratios are similar across broad geographic regions, reflecting intensive land-surface recycling
3. Monsoon water contributes minimally to runoff and groundwater recharge, its primary fate is evapotranspiration

Abstract

The North American monsoon (NAM) is an important source of precipitation across the southwestern United States (US). The approximate northern boundary of this feature crosses the Navajo Nation, in the Four Corners region, where NAM rains have long been important to the livelihoods of Native Americans. Relatively little is known about the characteristics and hydrological significance of the NAM in this region. Here we report a new 4-year record of stable H and O isotope ratios in monsoon-season rainfall and water resources across the Navajo Nation. Monthly precipitation samples collected at 39 sites document a characteristic pattern of ^{2}H- and ^{18}O-enrichment associated with monsoonal precipitation. These changes are weakly correlated with local precipitation intensity, however, and the correlation that does exist is dominated by sub-cloud evaporation effects. In contrast to precipitation amount, monsoon-season isotopic values exhibited limited spatial variability across the region, and after correction for sub-cloud evaporation Navajo Nation values were similar to those from a site in southern Arizona. Airmass back-trajectory analysis suggests that the uniformly high NAM isotope values across the region may reflect 1) a region-wide shift from mid-latitude to low-latitude moisture sources at the onset of the peak monsoon, and 2) substantial land-surface recycling of NAM moisture in upwind regions. Comparison of precipitation isotope data with surface and groundwater values implies that, despite its hydroclimatic significance, monsoon rainfall contributes little to rand subsurface water resources. This highlights the monsoon's importance for warm-season land-surface ecology and hydrology critical to residents of the Four Corners region.

Keywords

North American Monsoon, stable isotopes, Navajo Nation, water resources, climate change

1 Introduction

Past variability in precipitation across the arid southwestern United States has been documented over a range of time scales (Carleton et al., 1990; Gutzler, 2000; Ciancarelli et al., 2014; Carrillo et al., 2016), and both wet and dry extremes have been associated with environmental and societal impacts (Adams & Comrie, 1997). Seasonal precipitation within this region is bimodal, with a pronounced summer peak associated with winter synoptic systems originating from the North Pacific and a summer maximum reflecting the North American Monsoon (Carleton et al., 1990; Schmitz & Mullen, 1996; Adams & Comrie, 1997; Hu & Dominguez, 2015; Szejner et al., 2016; Tulley−Cordova et al., 2018). Although engineered water management systems across much of this region are designed to capture and store out-of-season water, and to ameliorate risks of extreme monsoon events, vast areas of rural land remain dependent on natural water resources and exposed to risk associated with their variability. Moreover, historic data and models suggest that increases in temperature-driven evaporation and changes in precipitation amounts and patterns have and will continue to reduce water availability in this region (Seager et al., 2007; Redsteer et al., 2010), and together with the potential for severe drought events (Cook et al., 2004) threaten sustainability of existing water infrastructure (Overpeck & Udall, 2010; Milly & Dunne, 2020).

The Diné Bikeyah, also known as the Navajo Nation ("NN"), spanning the "Four Corners" region of the current states of Utah, Colorado, New Mexico and Arizona, is the largest land-based Native American tribe in the United States, with an area over 70,000 square kilometers (Novak, 2007; Nania et al., 2014; Guiterman, 2015). Like many Indigenous peoples, the Navajo are particularly vulnerable to the impacts of climate change due to the arid environmental conditions across their homelands and their traditional ways of life (Redsteer et al., 2013; Wildcat, 2013; Nania et al., 2014; Bennett et al., 2017). The NN sits nearly the northern boundary of the modern NAM region. Annual average precipitation ranges from 67 mm in low-lying, northern areas to 738 mm in some high elevation areas (Tulley−Cordova et al., 2018). All areas of the NN experience a pronounced peak in precipitation during the summer associated with the NAM. This peak represents ~60%, on average, of annual precipitation in low-elevation areas and ~40% in in the mountains, but with substantial inter-annual variability (~20 to 80%) at all elevations (Tulley−Cordova et al., 2018). In most years, summer monsoon rains in the Four Corners region begin in July and extent through September, with peak rainfall occurring in July in the far eastern part of the region and August elsewhere.

Previous research has investigated the dynamics and history of the NAM across the broader southwestern USA. Modeling studies have highlighted two branches of the NAM, stemming from Gulf of California (GoC) and Gulf of Mexico (GoM), and associated their contributions to NAM rainfall with the depth and position of the low pressure system over the southwest (Carleton et al., 1990; Schmitz & Mullen, 1996; Adams & Comrie, 1997). Recycling of water from the land surface (through evaporation and transpiration) is thought to be a major source of moisture to monsoon precipitation across parts of the NAM region (Bosilovich, 2003; Hu & Dominguez, 2015). Hu & Dominguez (2015) also demonstrated a distinction between the isotopic composition of monsoon moisture derived from GoM (higher values) and Pacific/GoC sources (lower), suggesting that isotopes may be useful in reconstructing moisture transport patterns across the NAM region. Although their analysis did not clearly distinguish isotope values characteristic of recycled moisture, these authors present evidence that recycled moisture, which is accompanied by limited isotopic change (Ingraham & Taylor, 1991; Chamberlain et al., 2014), may preserve isotopic differences associated with different marine sources. Isotopic contrasts between NAM and winter precipitation in this region may also provide a basis for quantifying seasonal sources of water used by plants (Williams & Ehleringer, 2000) and, through isotopic measurements of proxies such as plant-derived biomarkers, reconstructing past variation in monsoon strength (Bhattacharya et al., 2018).

Despite our growing understanding of the NAM and its variability, projecting and planning for impacts of future NAM change requires additional work that further characterizes this feature of the hydroclimate and its impacts at local to regional scales relevant to management and policy. In this study we report and interpret a new 4-year monitoring record of precipitation and water resource H and O isotope values at sites across the NN. We characterize spatial and temporal isotopic patterns associated with NAM precipitation, evaluate the climatic processes that drive these patterns, and assess the contribution of NAM rainfall to water resources in this region. In addition to their relevance for understanding the modern NAM and its hydrological significance, these results should help inform future reconstructions of past NAM change based on isotopic proxy data.

2 Methods

2.1 Precipitation Monitoring

The precipitation gauge on the NN was installed in 1952. Since that time, the Navajo Nation Water Management Branch's Water Monitoring and Inventory Group (NNWMB) has managed over 190 precipitation gauges, as well as multiple snow survey and stream gaging sites, within their hydrometeorological network (Garfin et al., 2007; Aggett et al., 2011; Hart & Fisk, 2014;

Tsinnajinnie et al., 2018; Tulley−Cordova et al., 2018). The precipitation data from the NNWMB network documents regional hydroclimate across this large, remote region at a spatial extent and coverage not available from other methods (e.g., satellite and radar; Crimmins et al., 2013). Given the limited telecommunication and electrical infrastructure of the Four Corners region, data from most stations reflect total accumulations within rain cans, recorded manually at monthly intervals (Aggett et al., 2011; Tulley−Cordova et al., 2018).

2.2 Precipitation Sampling

We selected 39 sites from the NNWMB's hydrometeorological network for monthly precipitation collection and isotopic analysis (Figure 1). Samples were collected from May to October, 2014 to 2017. At two of the 39 sites (Fort Defiance, AZ and Rock Springs, NM), additional event-scale sampling was performed from May to October, 2015 to 2017. For the Rock Springs site, event-based sampling was extended through the winter months during 2016 and 2017 to produce a full-year record. A total of 1,084 precipitation samples were collected, and data were grouped for analysis into samples representing pre-monsoon (April – June), monsoon (July – September), and post-monsoon (including winter; October – March) seasons.

Precipitation was collected in custom-built devices consisting of a 10.2 cm diameter funnel connected to a 1 L, narrow mouth, Nalgene HDPE bottle using vinyl tubing and brass barb fittings. Silicone adhesive was used to secure and seal parts, and the collection tubing was extended to the bottom of the collection bottle to ensure that the bottom end was submerged after a small volume of precipitation had been collected. A small (2 mm) vent hole was drilled in the cap of the sample bottle to allow air from the bottle to escape as water entered. The collector was placed in a 66.0 cm long holder made from polyvinyl chloride (PVC) pipe, the bottom of which was buried and anchored in the ground. Following the 2014 collection season, several mL of mineral oil was added to each collector to prevent evaporation (2014 collections did not use oil, see discussion in the Results section).

Samples were collected at monthly intervals (monthly samples) or as soon as possible after precipitation events (event samples) and were weighed to determine the total precipitation amount (subtracting the combined weight of the bottle and mineral oil). We obtained an 8 mL aliquot of water (if available) from the bottle using a syringe, which was transferred to a glass rubber-seal sample bottle for storage. Samples from oil-containing collectors were filtered through a 0.45 um nylon syringe filter prior to storage. After sample collection, the collector bottle was replaced with a cleaned, dry bottle.

2.3 Water Resource Collection

We sampled a range of groundwater, lakes, and streams across the study area for stable isotopic analysis. All samples were collected in 4 mL glass vials with rubber lined closures, immediately capped, and the closure secured with Parafilm®. Groundwater samples (672) were gathered from 185 groundwater wells (Figure 1) in collaboration with Navajo Tribal Utility Authority (NTUA) drinking water compliance sampling conducted between March and September each year from 2014 to 2017. Lake samples were obtained from natural lakes and reservoirs by dip-sampling from the lake shore. Springs were sampled as close as possible to the point of discharge, either directly from a seep or from spring pools. Dip samples of ephemeral and perennial streams were collected from actively flowing parts of the stream. Each of these types of surface-collected samples were collected intermittently during the calendar year from 2014 to 2017. Overall, 58 lake, 116 stream, and 46 spring samples were obtained at 7, 25, and 45 sites, respectively (Figure 1).

2.4 Isotope Analysis

Samples were stored in a refrigerator at 4°C prior to analysis. Stable H and O isotope ratios were analyzed at the University of Utah Stable Isotope Ratios for Environmental Research (SIRFER) facility using a Cavity Ring-Down Spectroscopy instrument (Picarro L2130-i). All samples were calibrated to the Vienna Standard Mean Ocean Water (VSMOW) Standard Light Antarctic Precipitation (SLAP) reference scale based on data from co-analyzed reference waters (PZ: 16.9‰, 1.65‰; PT: −45.6‰, −7.23‰; UT: −123.1‰, −16.52‰; for δ^2H and $\delta^{18}O$, respectively). Sample values are reported in δ notation, where $\delta = R_{sample}/R_{standard} - 1$ and $R = {}^2H/{}^1H$ or ${}^{18}O/{}^{16}O$. Sample values represent an average of four replicate injections, with corrections applied for through-run drift and memory effects (Good et al., 2014).

To complement the NN data, we use published monthly-average precipitation isotope data collected in Tucson, Arizona (Eastoe & Dettman, 2016), which were accessed from the University of Arizona Environmental Isotope Laboratory Data Repository (https://www.geo.arizona.edu/node/154, accessed 12/18/2020). Values for individual months were averaged (without weighting) to obtain long-term average monthly values characterizing the annual cycle at Tucson.

2.5 Data Analysis

We use an updated version of the iSW_E (isotopic source water estimation with evaporation) model of Bowen et al. (2018) to assess the effect of post-condensation evaporation on precipitation samples and infer contributions of NAM and winter-season precipitation to surface and subsurface water resources. Briefly, the model predicts the measured isotopic composition (δ_{obs}) of a water sample from the values of an un-evaporated source water (δ_s) as:

$$\delta^{18}O_{obs} = \delta^{18}O_s + E\text{, and} \quad (1)$$

$$\delta^{2}H_{obs} = \delta^{2}H_s + E \times m, \quad (2)$$

where E is an evaporation index (in units of δ^{18}O ‰) and m is the slope of an evaporation line. Prior estimates are provided for each term on the right side of the equations, and the model is inverted using Bayes Rule to obtain a posterior distribution for all model parameters conditioned on the observed sample values. A uniform distribution bounded on 0 and 15‰ is used to evaluate a wider range of possible evaporation effect sizes, and a normal prior centered on 5 for all NN data and 4.8 for Tucson rainfall ($1\sigma = 0.3$) is used for the evaporation line slope based on the regional surface-water evaporation line values estimated by Bowen et al. (2018). The value of m is somewhat uncertain, and we tested the impact of using slightly different slope estimates (e.g., 5.5 ± 0.3); this produced only minor differences from the results presented here (not shown).

Prior estimates of the source values are specified in one of two ways. For analysis of pre-evaporation compositions of precipitation samples, the prior distribution is constrained by the statistics of the global meteoric water line (GMWL), representing the global mean covariant relationship between precipitation δ^2H and $\delta^{18}O$ values (Bowen et al., 2018). Although local deviations from this relationship can be expected due to vapor source characteristics (Putman et al., 2019), we prefer to characterize precipitation source values using the GMWL rather than a local meteoric water line estimated from ground-based precipitation sampling because of the potentially strong influence of sub-cloud re-evaporation of hydrometeors on the latter (see Results and Discussion). For analysis of surface and groundwater resources, source values are modeled as a linear mixture of two seasonal endmembers, each of which is represented by a bivariate normal distribution. The summer NAM endmember was approximated to reflect the variability among average NAM-season (July-September) precipitation isotope values at different monitoring sites (based on sampling from the observed averages with replacement); the distribution values for this endmember are -42, -5.7, 8.6, 1.8, and 14.5 (δ^2H, $\delta^{18}O$, δ^2H 1σ, $\delta^{18}O$ 1σ, and covariance, respectively). Since only a small number of winter precipitation data were collected, the endmember distribution was approximated by sampling three events from the individual data (November - March) with replacement and averaging; 10,000 such samples were drawn to characterize a distribution reflecting integration of event values but retaining a conservative (high) level of variability (parameter values: -82.9, -11.9, 14.2, 1.7, and 24.5). The prior estimate on the mixing model source values, then, was parameterized in terms of these endmember distributions and a NAM-source mixing fraction (f_{NAM}; winter faction = 1 - f_{NAM}) given by a Dirchlet distribution (shape parameters = [1,1]). We recognize that the isotopic endmembers are imperfectly characterized, particularly for winter precipitation, which adds potential uncertainty to the analysis. Subsequent work could address such factors as differences in the elevation and age of source-water recharge that might affect mixture estimates for some of these sample types; these factors are discussed where potentially relevant, below.

All data analysis was conducted in R version 4.0.2 (R Core Team, 2020). The functions used (*mwlSource* and *mixSource*) are available in version 0.2.1 of the *isoWater* package (Bowen, 2021), and conduct Markov Chain Monte Carlo sampling of the posterior distributions using rjags (Plummer, 2019) and R2jags (Su & Yajima, 2020). For all analyses, at least 200,000 samples were generated from each of three chains, with thinning to retain 2,500 samples per chain. Convergence was monitored using trace plots and the Gelman and Rubin convergence factor R-hat (Gelman & Rubin, 1992). We found that a burn-in period equal to 10% of the total chain length was adequate to remove any model initialization effects, and all analyses show moderate to strong convergence (R-hat < 1.03). Although the effective posterior sample size for analyses of some individual water samples was relatively small (~100), all interpretations drawn here are based on posterior samples from many (dozens if not hundreds) of water samples.

2.6 Back Trajectory Analysis

One documented control on precipitation stable isotope ratios is variation in vapor source region (Ichiyanagi & Yamanaka, 2005; Treble et al., 2005; Strong et al., 2007; Sodemann et al., 2008; Good et al., 2014; Putman, Feng, Sonder, et al., 2017). We evaluated the vapor source regions contributing to each pre-monsoon and monsoon season precipitation event sampled at Fort Defiance and Rock Springs in 2015-2017 using Lagrangian back trajectory analysis. Our analysis followed the procedure presented in Putman et al. (2017). In short, this method uses reanalysis data (https://www.ncdc.noaa.gov/data-access/model-data/model-datasets/global-data-assimilation-system-gdas) to estimate likely elevations of condensation, based on humidity, temperature and vertical velocity, and initiates air parcels at these heights. Because the exact time of precipitation for each event was unknown, a series of initiation times was evaluated to represent the most likely periods of the day for convective events typical of spring/summer NN rains. Parcels were first initialized at 12 Mountain Standard Time (MST), and if these failed to produce condensation a new set were initialized at 15 MST, followed by 18 MST, and 9 MST. For each analysis in which condensation occurred, 1000 back trajectories were initialized and tracked for 10 days (240 hours) back in time. Vapor sources were identified as locations where air parcels first intersected the boundary layer (as calculated from the reanalysis data).

Back trajectory analysis was also performed for July and August 2016 at two sites, Forest Lake, AZ and Smith Lake, NM, which are representative of the western and eastern seasonal precipitation regimes of the NN, respectively. No records of the timing of precipitation events were available for these sites, and back trajectories were initialized at both sites every day of July and August at 12, 3, and 6 MST. For each day and time, 500 air parcels were tracked 10 days (240 hours) back in time.

3 Results

3.1 Data Quality and Comparability

Summer conditions across the NN are severe, with temperatures often exceeding 35°C and limited precipitation accumulation. Although our precipitation collectors were designed to minimize potential for sample loss to evaporation, which directly affects isotope ratios, we conducted two activities to evaluate our success in this respect. From May to October, 2016, we deployed two identical precipitation collectors, one with and the other without mineral oil, at each of five monitoring sites distributed across the NN (Beaver Springs, AZ, Bluff, UT, Leupp, AZ, Nageezi, NM, and Rock Springs, NM). Aggregating the data by site or by month, there was no significant difference between the $\delta^{18}O$ values measured for the two methods (Table S1; paired T-test, all $p \geq 0.08$). What differences in the mean isotope ratios did exist were inconsistent, with the oil-free collectors giving slightly higher values, as would be expected to result from evaporative loss of sample water, in most, but not all cases. Likewise, there was no significant difference between the precipitation amounts measured for the two methods with the exception of the average across sites for May ($p = 0.04$), when the no-oil collectors recorded ~20% more precipitation than the collectors containing oil. This suggests that the addition or omission of oil, which has commonly been used to limit evaporation from rainfall collectors (Michelsen et al., 2018), had limited effect on our sample values.

As a second test, we compared data from event-based sampling, in which rainwater was collected as soon as possible (usually within 24 hours) after a precipitation event, with monthly-integrated samples at the two sites where both methods were used in parallel. After filtering for gaps in sampling and missing data, we identified 15 site-months between 2014 and 2017 for which a direct comparison could be made. We calculated precipitation amount-weighted average δ^2H and $\delta^{18}O$ values from the event-based samples. In cases where one or two event samples were missing sample amount information, we substituted the mean amount from other samples from the same site and month and flagged the resulting value of lower quality (4 site-months). Paired t-tests on the $\delta^{18}O$ data, conducted using all records or subsets that removed a single outlier value (July, 2014 at Fort Defiance), both 2014 (no-oil) measurements, or all low-quality data, showed no significant difference between event-based and monthly values (all $p > 0.08$).

Across all data, the monthly-integrated values were 1‰ higher, on average, than the event-based values, but this was driven primarily by the single outlier value. The two 2014 samples had the largest differences between monthly- and event-based values (11.0 and 2.5‰), and removing these from the sample-set the monthly-integrated sample values were 0.12‰ higher, on average, than the event-based values. Thus, the results of this test suggest that the long period (1-month) of integration used for the majority of our sampling resulted only minor post-precipitation isotope effects (if any), and that most of our measured values should be representative of unmodified precipitation to within a few tenths of a per mil. Although the sample numbers were small, this test, in contrast to the paired collector test describe above, suggests that the oil-free collectors used in 2014 may have allowed enough evaporative sample loss to substantially modify the isotopic values. Based on both lines of evidence, we retain the 2014 values in our analysis, but interpret them with caution in cases where post-collection evaporative effects might influence our interpretations.

3.2 Precipitation Isotope Data

Precipitation samples exhibit a wide range of values among sites and sampling periods (Fig. 2A-C). The mean values for monsoon season samples (-41.6 and -5.7‰ for δ^2H and $\delta^{18}O$, respectively) are highest, followed by those of pre-monsoon (-61.9 and -8.0‰) and post-monsoon (-66.7 and -9.5‰), respectively. Within each season, values are widely variable. Pre-monsoon precipitation values are most widely dispersed (1σ = 35.5 and 5.9‰), whereas monsoon season (21.6 and 3.6‰) and post-monsoon (21.7 and 3.2‰) variabilities are similar and lower. For each season, a large proportion of samples have values that plot near the global meteoric water line (GMWL: $\delta^2H = 8 \times \delta^{18}O + 10$), which is characteristic of most precipitation that has not experienced partial evaporation following condensation (Craig, 1961; Dansgaard, 1964). A substantial fraction of samples, however, particularly for the pre-monsoon and monsoon periods, plot well below the GMWL, as expected for samples that have experienced evaporation. Such samples are present in the data for all years, but are more common in some years and seasons (e.g., 2014 monsoon and post-monsoon, 2016 pre-monsoon, 2017 for all periods) than in others. As discussed in the previous section, we think it is unlikely that most samples experienced substantial evaporation after collection. In hot and dry conditions, such as those that characterize the NN throughout the spring-fall period, sub-cloud evaporation from falling raindrops is a common phenomenon, and is reflected in the isotopic composition of ground-collected rainfall (Gat, 1996; Kong et al., 2013; Salamalikis et al., 2016).

We used the iSW_E framework to estimate the pre-evaporation composition of each sample (Fig. 3A-C). The mean values for evaporation-corrected rainfall samples are substantially lower than the uncorrected values for all seasons (monsoon: -54.9 and -8.4‰; post-monsoon: -76.6 and -11.5‰; pre-monsoon: -78.1 and -11.3‰), and following correction the mean pre- and post-monsoon values are similar but remain distinct from the monsoon distribution. The convergence of the pre- and post-monsoon values reflects the greater degree of evaporation characteristic of the pre-monsoon samples, as shown by the iSW_E evaporation index (mean = 3.3, 2.7, and 2.0‰ for pre-monsoon, monsoon, and post-monsoon samples, respectively).

Navajo Nation hydroclimate varied substantially across the four study years, with 2015 being atypically wet throughout all seasons and 2014 featuring an atypically dry pre-monsoon period (Fig. 4). Despite this, the average monsoon-season precipitation isotope ratios were similar for all years. Individual year average pre- and post-monsoon values, both measured and evaporation-corrected, were much more variable than the monsoon-season values. Monsoon-season values were higher than pre- or post-monsoon for all years except 2016, when the pre-monsoon value was slightly higher than the monsoon-season average. Following evaporation correction, however, the 2016 pre-monsoon value was ~2‰ lower than the monsoon value, suggesting that the inversion of the pattern during that year reflected high rates of sub-cloud evaporation for the pre-monsoon samples. Relationships between individual-year seasonal-average precipitation amounts and isotope values were relatively weak. Prior to evaporation correction, monsoon period values were weakly, negatively correlated with precipitation amounts, with the lowest average value occurring during 2015. The post-monsoon values were weakly positively correlated with seasonal precipitation amounts (with or without evaporation-correction).

Across all years and samples, precipitation isotope ratios were weakly but significantly correlated with precipitation amount (as measured at the isotope sample collector) only for the pre-monsoon period and for all periods combined (Table 1). In both cases, H and O isotope values decreased with increasing precipitation amount, analogous to the "amount effect" that has long been observed at many tropical and subtropical monitoring sites (Dansgaard, 1964; Rozanski et al., 1993). For all sampling periods, however, the iSW_E evaporation index was significantly correlated with precipitation amount, indicating that the degree of post-condensation evaporative water loss increases during drier sampling periods (Table 1). The magnitude of this effect fully accounts for the observed isotope vs amount correlation for the combined (all periods) dataset, and explains approximately half of the observed correlation for the pre-monsoon data.

Limited spatial structure was observed in the stable isotope data, regardless of season. Monthly average values (across all 4 study years) for stations within each of the five seasonal hydroclimate cluster groups defined by Tulley-Cordova et al. (2018) exhibited similar patterns across the April-October period, and both patterns and values were very consistent across regions following evaporation correction (Fig. 5). Substantial differences that were observed between some regions for some months (e.g., April, June, and July) were largely attributable to differences in post-condensation evaporative effects, as reflected by the iSW_E evaporation index (Fig. 5C). The data, in particular the evaporation-corrected values, did show some subtle patterns that may reflect hydroclimatic influences. For example, the highest evaporation-corrected precipitation isotope ratios were observed in August for all site groups except the 'East' group, where values peaked in July and dropped by 1.8‰ in August. This difference corresponds with a difference in the timing of peak monsoon precipitation among regions, with precipitation peaking in August at sites in all groups except the East, and in July at the eastern sites (Tulley–Cordova et al., 2018).

Precipitation isotope ratios were weakly but significantly correlated with site elevation for all periods except the pre-monsoon (Table 2). The same was true of the iSW_E evaporation index. The strongest correlations were observed for the post-monsoon period, wherein site elevation explained up to 14% of the precipitation isotope variance (for $\delta^{18}O$). The slope of the isotope-elevation relationship for this period (-4.1‰/km for $\delta^{18}O$) was relatively high compared with other regions, globally (Poage & Chamberlain, 2001). A substantial fraction of the effect, however, can be attributed to post-condensation evaporation, which decreases with increasing site elevation by 2.1‰/km.

3.3 Back trajectory analysis

Of the 68 events sampled at Rock Springs and 60 events sampled at Fort Defiance between May and October, 2015-2017, back trajectories were successfully initiated for 60 and 54 events, respectively (Fig. 6). Premonsoon and monsoon vapor source regions differed. Premonsoon vapor sources tended to indicate land or Pacific origin vapor, typically traveling from the west into the region, whereas monsoon season vapor tended to indicate dominantly land-sourced vapor. Notably, monsoon season vapor included a large footprint over Mexico, as well as a smaller GoM source contribution. In a few instances, back trajectories indicate precipitation from large synoptic storm systems, carrying distal Pacific vapor into the region; such events are somewhat more common for the pre-monsoon than the monsoon period.

July and August trajectories at the Forest and Smith Lake sites suggest similar patterns of moisture origin, including major contributions from land surface recycling and additional input from the Pacific/GoC and GoM (Fig. 7). At the eastern site moisture sourced by strong southerly flow is somewhat reduced in August relative to July, whereas both southwesterly and (to a lesser degree) southeasterly flows continue to be the dominant source in August at Forest Lake (western NN).

3.4 Water resources

Isotope ratios of ground waters cluster near or just below the global meteoric water line and near the lower end of the range of precipitation sample values (Fig. 2D). Water resources sampled at the surface, including streams, springs, lake and reservoir samples, are somewhat more variable in their isotopic compositions, and include many samples that plot well below the GMWL (with relatively low d-excess values). This is particularly true for lake samples, most of which have low d-excess values and cluster along a line in δ^2H-δ^{18}O space that has a slope of ~5.5, similar to but slightly higher than that estimated for open-water evaporation in this region (Bowen et al., 2018). A small number of spring samples also have low d-excess values, possibly reflecting some amount of evaporative loss between the time of surface discharge and sample collection. The evaporation-corrected source water values for all sample types cluster tightly, and are relatively ^{2}H- and ^{18}O-depeleted relative to the distributions for precipitation samples (Fig. 3D).

The iSW$_E$ mixing model analysis suggests that the contribution of NAM precipitation to surface and groundwater resources is small (Fig. 8), consistent with the observation that most samples have relatively low isotopic values. The median contribution of NAM rain is estimated at 8%, 9%, 10%, and 16% for groundwater, springs, streams, and lakes, respectively. The somewhat higher estimated contribution of NAM precipitation to lake water may, in part, reflect the greater extent of evaporation for these samples (in that the larger evaporation correction is associated with greater uncertainty in source-water mixing estimates). This result, however, is relatively insensitive to the evaporation model assumptions used in our analysis (e.g., the median value differs by only 2% if a hypothesized evaporation line slope of 5.5 is adopted). The iSW$_E$ evaporation index distributions suggest that evaporative effects on lake-water δ^{18}O values are ~4x greater than those affecting any of the other water types (Fig. 8B).

4 Discussion

4.1 NAM precipitation isotopes

The new and extensive monitoring data collected here document the isotopic characteristics of NN NAM precipitation over space and time. Across the spring to fall season, these data show substantial, systematic temporal variability in precipitation isotopic compositions, but only weakly express correlative relationships with variables such as elevation and precipitation amount commonly observed at other sites. The relatively weak relationship with precipitation amount is perhaps unsurprising, as the study area lies outside of the low-latitude zone throughout which this mode of correlation is strongest (Bowen, 2008). Elevation effects, however, are widely observed in other regional precipitation studies (Poage & Chamberlain, 2001). We suggest that their weak expression here may in part relate to the localized and convective nature of NAM and shoulder-season precipitation, which may reduce the isotopic effect of rainout typically associated with orographic lifting of synoptic systems. The suggestion that orographic isotope effects are weaker for convective (vs. synoptic) systems is supported by the observation that isotope-elevation correlations in the NN data are strongest for the post-monsoon and full-year datasets, which encompass periods during which synoptic scale systems are likely to contribute substantially to precipitation.

Where precipitation amount and elevation correlations do exist in the NN data, our analysis suggests they are often associated with variation in post-condensation evaporation. Sub-cloud evaporation of falling raindrops is common in a wide range of meteorological settings characterized by low near-surface humidity and/or rainfall rates (Rindsberger et al., 1990; Worden et al., 2007; Mix et al., 2019) and its isotopic expression has previously been documented with the NAM (Quezadas et al., 2021). Our data suggest that the level of evaporation-drive enrichment of heavy isotopes in rainfall may vary systematically across seasons and sites. The strongest evaporation index values estimated here occurred during the dry and hot pre-monsoon season, producing measured rain sample values that approached or exceeded those of the monsoon season despite estimated pre-evaporation condensate values that were 4-8‰ lower than for NAM rains. The full extent of the observed isotope-precipitation amount correlations observed here, and half or more of the elevation effects, can be attributed to differences in evaporation among sites and sample periods (Tables 1 and 2). This highlights the potential for systematic variation in post-condensation effects to produce structured spatial and/or temporal variation in isotope ratios of precipitation arriving at the land surface.

The most distinctive feature of NN precipitation isotope data from the intensively sampled spring-to-fall period is the pronounced maximum during the peak monsoon months of July and August (Fig. 5). Across the study region, monthly mean $\delta^{18}O$ values for this period are typically between -3 and -6‰. Outside of the peak monsoon season, values in this range are rare, and are generally associated with a high degree of post-condensation evaporation, implying that the isotope values for atmospheric moisture transported to the NN during the peak of the NAM are substantially higher than those during the immediate pre-and post-monsoon periods (Fig. 5B). This pattern differs from that observed for precipitation in Tucson, AZ, some 400 km to the south, where ground-collected precipitation $\delta^{18}O$ values, and even more so evaporation-corrected values, remain relatively stable from April or May through October (Fig. 5). Moreover, precipitation isotope values for the NN and Tucson converge and are nearly identical during the peak monsoon months, despite the large difference in proximity to marine moisture sources for these two areas.

We suggest that the convergence between NN and Tucson precipitation isotope ratios during the peak NAM reflects substantial sub-cloud and land-surface moisture recycling during the propagation of NAM moisture to the Four Corners Region. Recycling returns moisture to the atmosphere with similar, or higher, isotope ratios than those of the precipitation source, diminishing or eliminating coast-to-continent gradients otherwise typically associated with the progressive rainout of vapor from air masses (Gat & Matsui, 1991; Ingraham & Taylor, 1991; Winnick et al., 2014). Land-surface recycling has previously been identified as a prominent mechanism for the propagation of NAM rains to the continental interior (Dominguez & Kumar, 2008), and will be discussed further below. Sub-cloud evaporation of falling droplets, discussed above, is a second mechanism which can reduce isotope effects associated with rainout (Worden et al., 2007), and is clearly implicated within the dataset examined here based on the relatively large evaporation effects estimated from both NN and Tucson precipitation samples (though perhaps of reduced significance during the peak NAM months; Fig. 5C). We suggest that as the monsoonal circulation intensifies, the penetration of moisture to the northern reaches of the NAM is accompanied and facilitated by high rates of sub-cloud and land-surface recycling, which also drives a large increase in the $\delta^{18}O$ values of NN precipitation and a collapse of the isotopic gradient between this region and upwind, source-proximal areas. Further to the north, at Cedar City, UT, isotope ratios of summer rainfall associated with NAM-like circulation ($\delta^{18}O \approx -8.5$‰) are higher than those associated with other circulation trajectories but somewhat lower than NN NAM season values (Friedman et al., 2002). This area lies outside of the core NAM region, and the net rainout from the relatively rare and weak monsoon-associated events arriving at Cedar City is likely greater, with a larger isotopic impact, than at the NN.

An additional potential source of variation in NAM-season precipitation isotope ratios is differences or changes in the balance of water arriving from different moisture sources (Hu & Dominguez, 2015). The increase in precipitation isotope values characterizing the onset of the monsoon season is associated with a shift from mid-latitude oceanic and continental moisture sources to GoM and Pacific/GoC sources and subtropical continental sources associated with circulation off of these oceanic regions (Fig. 6). Onset of high-δ^2H and δ^{18}O moisture transport from these warm oceanic sources, then, combined with strong recycling from upwind continental regions, likely drives the seasonal isotopic maximum associated with the NAM. Trajectory analysis within the monsoon season suggests that moisture transport from the southeast, including GoM sources, declines first (in August) in the eastern NN (Fig. 7), coincident with the earlier weakening of NAM rains in that region than across the rest of the NN (Tulley−Cordova et al., 2018). Weaker August precipitation in the eastern NN appears to be sourced primarily from the southwest/GoC, with secondary additions from the continental interior, and the lower isotope ratios characteristic of these sources may explain the early decline in evaporation-corrected isotope values in this region during August, the month when maximum values are reached elsewhere across the NN (Fig. 5).

Although proxy data recording the isotopic composition of ancient precipitation have been widely used to reconstruct continental paleoclimate, growing recognition that controls on variation in precipitation isotope ratios are diverse and variable has required re-thinking traditional approaches to this work (Schmidt et al., 2007; Liu et al., 2010; Chamberlain et al., 2014; Putman et al., 2021). Our characterization of NAM and shoulder-season precipitation from the Four Corners suggests that controls on isotope ratios in this region are diverse and likely include changes in moisture source, land surface recycling in upwind regions, and local sub-cloud evaporation. Although our monitoring spanned only four years, substantial differences in hydroclimate particularly within the pre- and post-monsoon seasons, occurred within that window of time. In general, the variability in isotope values between monitoring sites in a given year greatly exceeded the variability in mean NN values across years (Fig. 4), suggesting that extraction of paleoclimate records from precipitation isotope proxy data in this region may be challenging. A possible exception is the inverse correlation between precipitation amounts and isotope ratios, driven by differences in sub-cloud evaporation, which is strongly expressed in the pre-monsoon season (Fig. 4, Table 1). Although it is unlikely that most proxy records would directly reflect isotope ratios of water from this season, the pattern observed here may reflect a more general mechanism by which variation in warm season precipitation intensity is expressed in rainfall isotope ratios and could be reconstructed from proxy data.

4.2 Fate of NAM water

Another common application of precipitation isotope data is in quantifying the contribution of different precipitation sources to plants, animals, or water resources. Here, we investigated the contribution of NAM and post-monsoon (winter) season precipitation to a range of water resources that are essential to the people and ecosystems of the NN. We found that, although the NAM contributes approximately 50% of total annual precipitation across most of the study area, its contribution to surface and groundwater resources was minimal, constituting only ~10% of total inputs, on average (Fig. 8). This result is consistent with isotope-based estimates from springs in the Grand Canyon region of Northern Arizona (Solder & Beisner, 2020), also near the northern margin of the NAM west of our study area. A small number of ephemeral stream samples are exceptions to this pattern, likely reflecting direct runoff of NAM rainfall, and estimated contributions from highly-evaporated lakes and reservoirs are relatively uncertain and allow for somewhat higher NAM contributions.

Despite accounting for multiple sources of uncertainty, the isotope mass balance estimates calculated here are admittedly approximate. The limitations of our approach include relatively sparse sampling of cool-season precipitation and the potential that recharge includes a substantial fraction of high-elevation or ancient precipitation that is not adequately represented in the isotopic endmembers used here. Nonetheless, our measured values for a range of water types are uniformly much lower than those of NAM precipitation (Fig. 2). Even if some water resource samples were partially derived from another (e.g., high-elevation winter or paleowater) source with substantially lower isotope ratios than the winter source measured here, a substantial contribution from NAM rainfall seems unlikely. Accounting for a 50:50 NAM:winter mixture in a typical surface water sample with $\delta^{18}O$ = -13‰ (and assuming the NAM endmember described in our Methods) would require a mean winter season precipitation value of -20.3‰. Using a typical North American isotopic lapse rate of 2.8‰/km (Poage & Chamberlain, 2001; Dutton et al., 2005), this would imply an implausible mean recharge elevation 3 km higher than our monitoring site (itself at 2007 m).

Our evidence for a limited contribution of NAM rainfall to surface and subsurface water resources on the NN is perhaps not surprising, and does not imply that these rains are hydrologically unimportant. Previous isotopic work has demonstrated substantial uptake and transpiration of monsoon rainfall by many plant species in this region (Williams & Ehleringer, 2000; Williams et al., 2005; English et al., 2007). Moreover, our rainfall data discussed above provides evidence for rainfall re-evaporation and for a large fraction of regional summer rainfall being returned to the atmosphere as evapotranspiration (inferred from weak gradients in precipitation isotope ratios across the NAM region). Together, these lines of evidence point to land-atmosphere flux as the primary fate for NAM precipitation in this region, consistent with, and supported by, the lack of evidence for significant monsoon recharge of surface or subsurface water resources.

5 Conclusions

Our new data document spatial, temporal, and water resource-related patterns of water H and O stable isotope values across the sparsely sampled Four Corners region of the southwestern United States. We identify variation in atmospheric water sources and post-condensation evaporation as two primary drivers of warm season (spring through fall) precipitation isotope ratio change, and suggest that a shift to low-latitude vapor sources combined with very strong land-surface recycling in upwind areas combine to produce the prominent isotopic maximum associated with North American Monsoon rainfall. Our analysis suggests that NAM rainfall, though volumetrically significant, contributes minimally to regional ground and surface water resources. Instead, we argue that the primary fate for NAM precipitation is re-evaporation (and transpiration). Groundwaters, lakes, streams, and springs located in this region are thus unlikely to be strongly sensitive to future changes in the North American monsoon, but impacts of monsoon change on plant species that are adapted to use summer rains and on water recycling feedbacks that can sustain and propagate NAM-derived moisture to the continental interior (e.g., Dominguez et al., 2009) may be more significant.

Acknowledgments

The authors thank the Navajo Nation Water Management Branch's Water Monitoring and Inventory Section, especially Irving Brady, Jerome Bekis, Linda Lee, and Carlee McClellan, Navajo Tribal Utility Authority, particularly Raquel Whitehorse, Navajo citizen scientists, and Tulley and Cordova families who assisted with stable isotopic sample collections. This research has been supported by grant FP-917808 from the U.S. Environmental Protection Agency's Science to Achieve Results (STAR) Program, the Navajo Nation, the Intertribal Timber Council and United States Forest Service's Native American Natural Resources Research Scholarship, the University of Utah's Global Change and Sustainability Center's Research Grant, and US National Science Foundation Grant DEB-1802880. Any opinions, findings, conclusions, or recommendations expressed in this material are those of the authors and do not necessarily reflect the views of the funding agencies. The new water isotope data analyzed in this study are deposited in and were obtained from the Waterisotopes Database (https://waterisotopesDB.org, query: Project = '00066') and all isotope and precipitation data, data processing scripts, and code used to generate figures 2-5 and 8 are archived with Zenodo (https://doi.org/10.5281/zenodo.4628328).

References

Adams, D. K., & Comrie, A. C. (1997). The north American monsoon. *Bulletin of the American Meteorological Society, 78*(10), 2197-2214.

Aggett, G., Frisbee, M., Harding, B., Miller, G. H., & Weil, P. (2011). *Hydromet Network Optimization for the Navajo Nation's Department of Water Resources Water Management Branch*. Retrieved from

Bennett, T., Maynard, N. G., Cochran, P., Gough, R., Lynn, K., Maldonado, J., . . . Cozzetto, K. (2017). Ch. 12: Indigenous peoples, lands, and resources. In J. Melillo, T. Richmond, & G. Yohe (Eds.), *Climate Change Impacts in the United States: The Third National Climate Assessment* (pp. 297-317): U.S. Global Change Research Program.

Bhattacharya, T., Tierney, J. E., Addison, J. A., & Murray, J. W. (2018). Ice-sheet modulation of deglacial North American monsoon intensification. *Nature Geoscience, 11*(11), 848-852.

Bosilovich, M. G. (2003). Numerical simulation of the large-scale North American monsoon water sources. *108*(D16). doi:10.1029/2002jd003095

Bowen, G. J. (2008). Spatial analysis of the intra-annual variation of precipitation isotope ratios and its climatological corollaries. *Journal of Geophysical Research, 113, D05113*. doi:10.1029/2007JD009295

Bowen, G. J. (2021). SPATIAL-Lab/isoWater: Paria (Version 0.2.1). doi:10.5281/zenodo.4599209

Bowen, G. J., Putman, A., Brooks, J. R., Bowling, D. R., Oerter, E. J., & Good, S. P. (2018). Inferring the source of evaporated waters using stable H and O isotopes. *Oecologia, 187*, 1025-1039. doi:10.1007/s00442-018-4192-5

Carleton, A. M., Carpenter, D. A., & Weser, P. J. (1990). Mechanisms of interannual variability of the southwest United States summer rainfall maximum. *Journal of Climate, 3*(9), 999-1015.

Carrillo, C. M., Castro, C. L., Woodhouse, C. A., & Griffin, D. (2016). Low−frequency variability of precipitation in the North American monsoon region as diagnosed through earlywood and latewood tree−ring chronologies in the southwestern US. *International Journal of Climatology, 36*(5), 2254-2272.

Chamberlain, C. P., Winnick, M. J., Mix, H. T., Chamberlain, S. D., & Maher, K. (2014). The impact of Neogene grassland expansion and aridification on the isotopic composition of continental precipitation. *Global Biogeochemical Cycles*, 2014GB004822. doi:10.1002/2014GB004822

Ciancarelli, B., Castro, C. L., Woodhouse, C., Dominguez, F., Chang, H. I., Carrillo, C., & Griffin, D. (2014). Dominant patterns of US warm season precipitation variability in a fine resolution observational record, with focus on the southwest. *International Journal of Climatology, 34*(3), 687-707.

Cook, E. R., Woodhouse, C. A., Eakin, C. M., Meko, D. M., & Stahle, D. W. (2004). Long-term aridity changes in the western United States. *Science, 306*, 1015-1018.

Craig, H. (1961). Isotopic variations in meteoric waters. *Science, 133*, 1702-1703.

Crimmins, M. A., Selover, N., Cozzetto, K., & Chief, K. (2013). *Technical Review of the Navajo Nation Drought Contingency Plan - Drought Monitoring*. Retrieved from http://www.climas.arizona.edu/publication/report/technical-review-navajo-nation-drought-contingency-plan-drought-monitoring

Dansgaard, W. (1964). Stable isotopes in precipitation. *Tellus, 16*(4), 436-468.

Dominguez, F., & Kumar, P. (2008). Precipitation recycling variability and ecoclimatological stability-A study using NARR data. Part II: North American Monsoon Region. *Journal of Climate, 21*, 5187-5203. doi:10.1175/2008JCLI1760.1

Dominguez, F., Villegas, J. C., & Breshears, D. D. (2009). Spatial extent of the North American Monsoon: Increased cross-regional linkages via atmospheric pathways. *Geophysical Research Letters, 36, L07401*. doi:10.1029/2008GL037012

Dutton, A., Wilkinson, B. H., Welker, J. M., Bowen, G. J., & Lohmann, K. C. (2005). Spatial distribution and seasonal variation in $^{18}O/^{16}O$ of modern precipitation and river water across the conterminous United States. *Hydrological Processes, 19*, 4121-4146. doi:10.1002/hyp.5876

Eastoe, C. J., & Dettman, D. L. (2016). Isotope amount effects in hydrologic and climate reconstructions of monsoon climates: Implications of some long-term data sets for precipitation. *Chemical Geology, 430*, 78-89. doi:http://dx.doi.org/10.1016/j.chemgeo.2016.03.022

English, N. B., Dettman, D. L., Sandquist, D. R., & Williams, D. G. (2007). Past climate changes and ecophysiological responses recorded in the isotope ratios of saguaro cactus spines. *Oecologia, 154*, 247-258.

Friedman, I., Harris, J. M., Smith, G. I., & Johnson, C. A. (2002). Stable isotope composition of waters in the Great Basin, United States 1. Air-mass trajectories. *Journal of Geophysical Research, 107*(D19), 4400. doi:10.1029/2001JD000565

Garfin, G. M., Ellis, A., Selover, N., Anderson, D. M., Tecle, A., Heinrich, P., . . . Harvey, C. (2007). *Assessment of the Navajo Nation Hydroclimate Network*. Retrieved from https://www.climas.arizona.edu/sites/default/files/pdfnavajo-hydromet-assess-2007.pdf

Gat, J. R. (1996). Oxygen and Hydrogen Isotopes in the Hydrologic Cycle. *Annual Review of Earth and Planetary Sciences, 24*, 225-262.

Gat, J. R., & Matsui, E. (1991). Atmospheric water balance in the Amazon Basin: an isotopic evapotranspiration model. *Journal of Geophysical Research, 96*, 13,179-113,188.

Gelman, A., & Rubin, D. B. (1992). Inference from iterative simulation using multiple sequences. *Statistical Science, 7*(4), 457-472.

Good, S. P., Mallia, D. V., Lin, J. C., & Bowen, G. J. (2014). Stable Isotope Analysis of Precipitation Samples Obtained via Crowdsourcing Reveals the Spatiotemporal Evolution of Superstorm Sandy. *PLoS ONE, 9*(3), e91117. doi:10.1371/journal.pone.0091117

Guiterman, C. H. (2015). *Climatic sensitivities of Navajo forestlands: Use-inspired research to guide tribal forest management*. Retrieved from University of Arizona, Tucson, AZ: http://www.climas.arizona.edu/sites/default/files/pdfclimas-fellow-finalreport2014guiterman.pdf

Gutzler, D. S. (2000). Covariability of spring snowpack and summer rainfall across the southwest United States. *Journal of Climate, 13*(22), 4018-4027.

Hart, R. J., & Fisk, G. G. (2014). *Field Manual for the Collection of Navajo Nation Streamflow-Gage Data*: US Department of the Interior, US Geological Survey Open-File Report 2013-1107.

Hu, H., & Dominguez, F. (2015). Evaluation of Oceanic and Terrestrial sources of moisture for the North American Monsoon using Numerical Models and Precipitation Stable Isotopes. *Journal of Hydrometeorology, 16*, 19-35.

Ichiyanagi, K., & Yamanaka, M. D. (2005). Interannual variation of stable isotopes in precipitation at Bangkok in response to El Ñino Southern Oscillation. *Hydrological Processes, 19*(17), 3413-3423. doi:10.1002/hyp.5978

Ingraham, N. L., & Taylor, B. E. (1991). Light stable isotope systematics of large-scale hydrologic regimes in California and Nevada. *Water Resources Research, 27*(1), 77-90.

Kong, Y., Pang, Z., & Froehlich, K. (2013). Quantifying recycled moisture fraction in precipitation of an arid region using deuterium excess. *Tellus B: Chemical and Physical Meteorology, 65*(1), 19251. doi:10.3402/tellusb.v65i0.19251

Liu, Z., Bowen, G. J., & Welker, J. M. (2010). Atmospheric circulation is reflected in precipitation isotope gradients over the conterminous United States. *Journal of Geophysical Research, 115, D22120*. doi:10.1029/2010JD014175

Michelsen, N., Van Geldern, R., Roßmann, Y., Bauer, I., Schulz, S., Barth, J. A. C., & Schüth, C. (2018). Comparison of precipitation collectors used in isotope hydrology. *Chemical Geology, 488*, 171-179. doi:10.1016/j.chemgeo.2018.04.032

Milly, P. C. D., & Dunne, K. A. (2020). Colorado River flow dwindles as warming-driven loss of reflective snow energizes evaporation. *Science, 367*(6483), 1252-1255. doi:10.1126/science.aay9187

Mix, H., Reilly, S., Martin, A., & Cornwell, G. (2019). Evaluating the Roles of Rainout and Post-Condensation Processes in a Landfalling Atmospheric River with Stable Isotopes in Precipitation and Water Vapor. *Atmosphere, 10*(2), 86. doi:10.3390/atmos10020086

Nania, J., Cozzetto, K., Gillett, N., Druen, S., Tapp, A. M., Eitner, M., . . . Assessment, W. W. (2014). *Considerations for climate change and variability adaptation on the Navajo*

Nation. Retrieved from University of Colorado, Boulder, Colorado: https://wwa.colorado.edu/publications/reports/navajo_report4_9.pdf

Novak, R. M. (2007). *Climate variability and change in the Chuska Mountain area: Impacts, information, and the intersection of western science and traditional knowledge.* (M.S.). University of Arizona, Tucson, Arizona. Retrieved from https://www.geo.arizona.edu/Antevs/Theses/NovakMS2007.pdf

Overpeck, J., & Udall, B. (2010). Dry times ahead. *Science, 328*(5986), 1642-1643.

Plummer, M. (2019). rjags: Bayesian graphical models using MCMC. R package version 4-10. https://CRAN.R-project.org/package=rjags. Retrieved from https://CRAN.R-project.org/package=rjags

Poage, M. A., & Chamberlain, C. P. (2001). Empirical relationships between elevation and the stable isotope composition of precipitation and surface waters: Considerations for studies of paleoelevation change. *American Journal of Science, 301*(1), 1-15.

Putman, A. L., Bowen, G. J., & Strong, C. (2021). Local and regional modes of hydroclimatic change expressed in modern multidecadal precipitation oxygen isotope trends. *Geophysical Research Letters, 48*(5). doi:10.1029/2020gl092006

Putman, A. L., Feng, X., Posmentier, E. S., Faiia, A. M., & Sonder, L. J. (2017). Testing a Novel Method for Initializing Air Parcel Back Trajectories in Precipitating Clouds Using Reanalysis Data. *Journal of Atmospheric and Oceanic Technology, 34*(11), 2393-2405. doi:10.1175/jtech-d-17-0053.1

Putman, A. L., Feng, X., Sonder, L. J., & Posmentier, E. S. (2017). Annual variation in event-scale precipitation δ^2H at Barrow, AK, reflects vapor source region. *Atmospheric Chemistry and Physics, 17*(7), 4627-4639.

Putman, A. L., Fiorella, R. P., Bowen, G. J., & Cai, Z. (2019). A global perspective on local meteoric water lines: Meta−analytic insight into fundamental controls and practical constraints. *Water Resources Research, 55*(8), 6896-6910.

Quezadas, J. P., Adams, D., Sánchez Murillo, R., Lagunes, A. J., & Rodríguez Castañeda, J. L. (2021). Isotopic variability ($\delta^{18}O$, $\delta^{2}H$ and d-excess) during rainfall events of the north American monsoon across the Sonora River Basin, Mexico. *Journal of South American Earth Sciences, 105*, 102928. doi:10.1016/j.jsames.2020.102928

R Core Team. (2020). R: A language and environment for statistical computing. *R Foundation for Statistical Computing, Vienna, Austria. https://www.R-project.org/*.

Redsteer, M. H., Bemis, K., Chief, K., Gautam, M., Middleton, B. R., Tsosie, R., & Ferguson, D. B. b. (2013). Unique challenges facing southwestern tribes. In *Assessment of climate change in the southwest United States* (pp. 385-404): Springer.

Redsteer, M. H., Kelley, K. B., Francis, H., & Block, D. (2010). Disaster risk assessment case study: Recent drought on the Navajo nation, southwestern United States. In *2011 global assessment report on disaster risk reduction* (pp. 1-19). Geneva, Switzerland: United Nations Office for Disaster Risk Reduction.

Rindsberger, M., Jaffe, S., Rahamim, S., & Gat, J. (1990). Patterns of the isotopic composition of precipitation in time and space: data from the Israeli storm water collection program. *Tellus B, 42*(3), 263-271.

Rozanski, K., Araguás-Araguás, L., & Gonfiantini, R. (1993). Isotopic patterns in modern global precipitation. In *Climate Change in Continental Isotopic Records* (Vol. 78, pp. 1-36). Washington, DC: AGU.

Salamalikis, V., Argiriou, A. A., & Dotsika, E. (2016). Isotopic modeling of the sub-cloud evaporation effect in precipitation. *Science of The Total Environment, 544*, 1059-1072. doi:10.1016/j.scitotenv.2015.11.072

Schmidt, G. A., LeGrande, A. N., & Hoffmann, G. (2007). Water isotope expressions of intrinsic and forced variability in a coupled ocean-atmosphere model. *Journal of Geophysical Research, 112, D10103*. doi:10.1029/2006JD007781

Schmitz, J. T., & Mullen, S. L. (1996). Water vapor transport associated with the summertime North American monsoon as depicted by ECMWF analyses. *Journal of Climate, 9*(7), 1621-1634.

Seager, R., Ting, M. F., Held, I., Kushnir, Y., Lu, J., Vecchi, G., . . . Naik, N. (2007). Model projections of an imminent transition to a more arid climate in southwestern North America. *Science, 316*(5828), 1181-1184. Retrieved from <Go to ISI>://000246724300040

Sodemann, H., Masson-Delmotte, V., Schwierz, C., Vinther, B. M., & Wernli, H. (2008). Interannual variability of Greenland winter precipitation sources: 2. Effects of North Atlantic Oscillation variability on stable isotopes in precipitation. *Journal of Geophysical Research: Atmospheres, 113*(D12). doi:doi:10.1029/2007JD009416

Solder, J. E., & Beisner, K. R. (2020). Critical evaluation of stable isotope mixing end-members for estimating groundwater recharge sources: Case study from the South Rim of the Grand Canyon, Arizona, USA. *Hydrogeology Journal, 28*, 1575-1591. doi:10.1007/s10040-020-02194-y

Strong, M., Sharp, Z. D., & Gutzler, D. S. (2007). Diagnosing moisture transport using D/H ratios of water vapor. *Geophysical Research Letters, 34, L03404*, 1-5. doi:10.1029/2006GL028307

Su, Y.-S., & Yajima, M. (2020). R2jags: Using R to Run 'JAGS'. R package version 0.6-1. https://CRAN.R-project.org/package=R2jags.

Szejner, P., Wright, W. E., Babst, F., Belmecheri, S., Trouet, V., Leavitt, S. W., . . . Monson, R. K. (2016). Latitudinal gradients in tree ring stable carbon and oxygen isotopes reveal differential climate influences of the North American Monsoon System. *Journal of Geophysical Research: Biogeosciences, 121*(7), 1978-1991.

Treble, P. C., Chappell, J., Gagan, M. K., McKeegan, K. D., & Harrison, T. M. (2005). In situ measurement of seasonal $d^{18}O$ variations and analysis of isotopic trends in a modern speleothem from southwest Australia. *Earth & Planetary Science Letters, 233*, 17-32. doi:doi:10.1016/j.epsl.2005.02.013

Tsinnajinnie, L. M., Gutzler, D. S., & John, J. (2018). Navajo Nation Snowpack Variability from 1985-2014 and Implications for Water Resources Management. *Journal of Contemporary Water Research & Education, 163*(1), 124-138. doi:10.1111/j.1936-704x.2018.03274.x

Tulley−Cordova, C. L., Strong, C., Brady, I. P., Bekis, J., & Bowen, G. J. (2018). Navajo Nation, USA, Precipitation Variability from 2002 to 2015. *Journal of Contemporary Water Research and Education, 163*(1), 109-123.

Wildcat, D. R. (2013). Introduction: climate change and indigenous peoples of the USA. *Climatic Change, 120*(3), 509-515. doi:10.1007/s10584-013-0849-6

Williams, D. G., Coltrain, J. B., Lott, M. J., English, N. B., & Ehleringer, J. R. (2005). Oxygen isotopes in cellulose identify source water for archaeological maize in the American

Southwest. *Journal of Archaeological Science, 32*(6), 931-939. doi:10.1016/j.jas.2005.01.008

Williams, D. G., & Ehleringer, J. R. r. (2000). Intra- and interspecific variation for summer precipitation use in pinyon-juniper woodlands. *Ecological Monographs, 70*(4), 517-537.

Winnick, M. J., Chamberlain, C. P., Caves, J. K., & Welker, J. M. (2014). Quantifying the isotopic ‘continental effect’. *Earth and Planetary Science Letters, 406*, 123-133.

Worden, J., Noone, D., Bowman, K., Beer, R., Eldering, A., Fisher, B., . . . Worden, H. (2007). Importance of rain evaporation and continental convection in the tropical water cycle. *Nature, 445*, 528-532. doi:10.1038/nature05508

Table 1: Linear regression statistics describing the correlation between precipitation isotope values and precipitation amount (in mm; bold: $p < 0.05$).

Period	δ^2H vs Amount		$\delta^{18}O$ vs Amount		Evaporation vs Amount	
	Slope	R^2	Slope	R^2	Slope	R^2
All	**-0.135**	**0.012**	**-0.042**	**0.048**	**-0.046**	**0.121**
Pre-monsoon	**-1.018**	**0.265**	**-0.172**	**0.262**	**-0.078**	**0.124**
Monsoon	-0.126	0.019	-0.035	0.057	**-0.037**	**0.113**
Post-monsoon	0.158	0.023	-0.017	0.005	**-0.06**	**0.184**

Table 2: Linear regression statistics describing the correlation between precipitation isotope values and site elevation (in km; bold: $p < 0.05$).

Period	δ^2H vs Elevation		$\delta^{18}O$ vs Elevation		Evaporation vs Elevation	
	Slope	R^2	Slope	R^2	Slope	R^2
All	**-9.7**	**0.01**	**-2.1**	**0.018**	**-1.4**	**0.018**
Pre-monsoon	-5.6	0	-1.3	0.001	-0.6	0
Monsoon	**-6.8**	**0.007**	**-1.7**	**0.019**	**-1.6**	**0.031**
Post-monsoon	**-21.4**	**0.08**	**-4.1**	**0.139**	**-2.1**	**0.048**

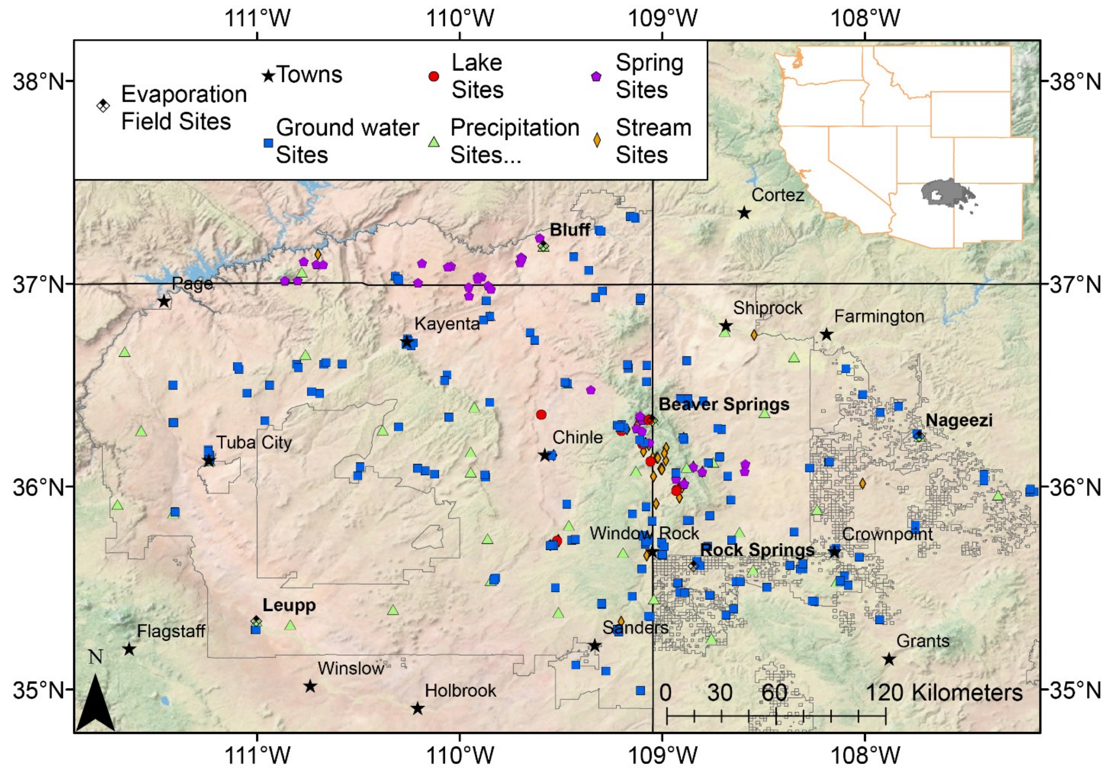

Figure 4. Sampling sites within the boundaries of the Navajo Nation (grey lines). Bold names denote evaporation experiment field sites.

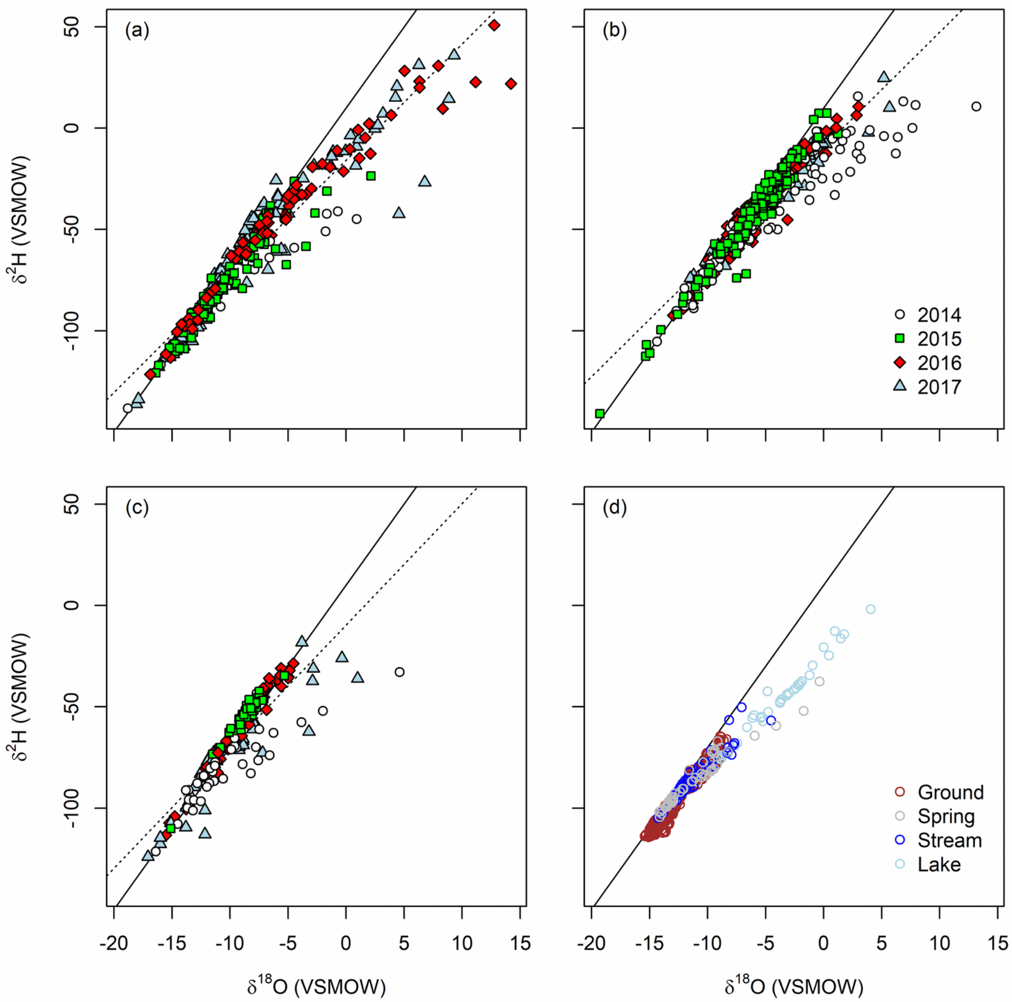

Figure 2: Stable H and O isotope ratios of water samples from the Navajo Nation. Panels show precipitation from (a) pre-monsoon, (b) monsoon, or (c) post-monsoon seasons, and from surface and groundwater samples (d). Dotted lines are regressions through each dataset (a-c), and the solid line in each panel shows the Global Meteoric Water Line.

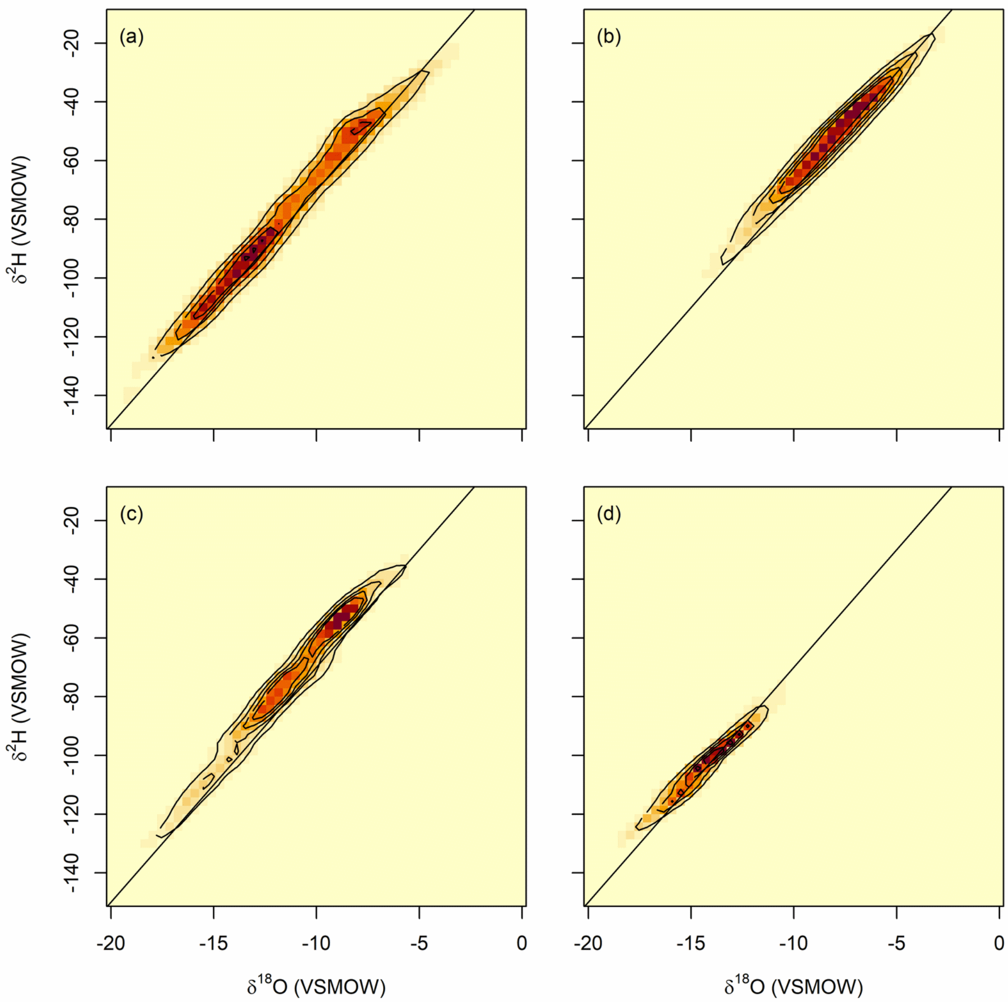

Figure 3: 2-dimensional density plots showing the distribution of water isotope values for Navajo Nation samples following correction for post-condensation evaporation effects. Panels show distributions for (a) pre-monsoon, (b) monsoon, and (c) post-monsoon precipitation and (d) surface and subsurface water resources. Colors are proportional to the density of source water isotope values in the posterior distribution of the iSW_E analysis, and contours separate density values at intervals of 0.2% in A-C and 0.6% in (d). The solid line in each panel shows the Global Meteoric Water Line.

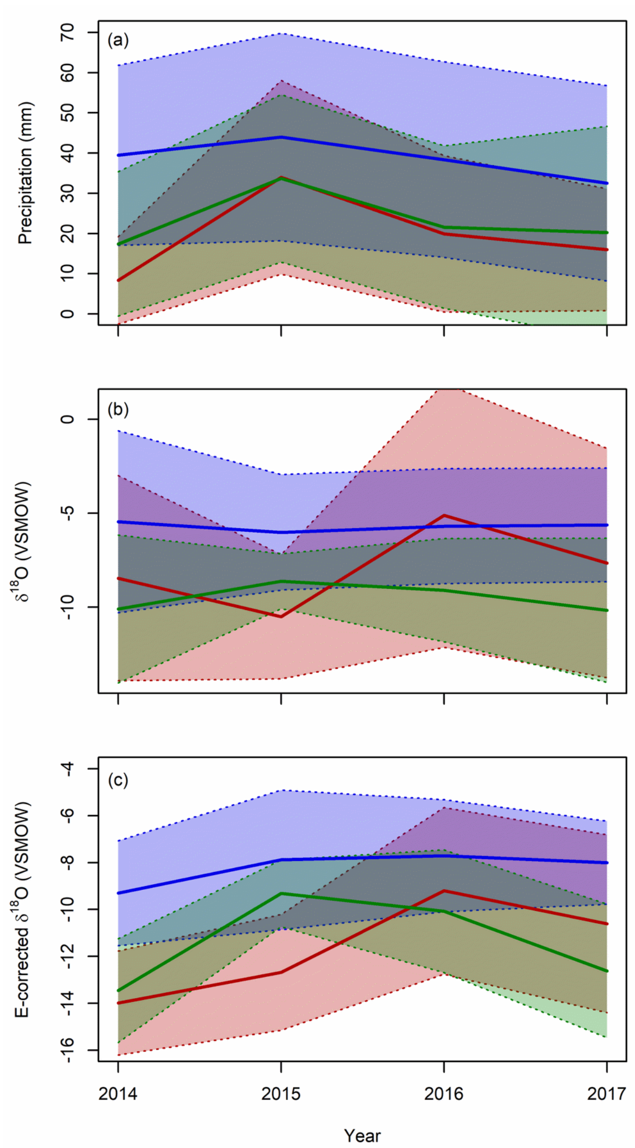

Figure 4: Inter-annual trends in seasonal precipitation and isotope data across the Navajo Nation, showing mean values and 1σ ranges for pre-monsoon (red), monsoon (blue), and post-monsoon (green) months. Panels show precipitation amount (a), measured precipitation $\delta^{18}O$ values (b), and precipitation O-isotope values corrected for post-condensation evaporation effects (c).

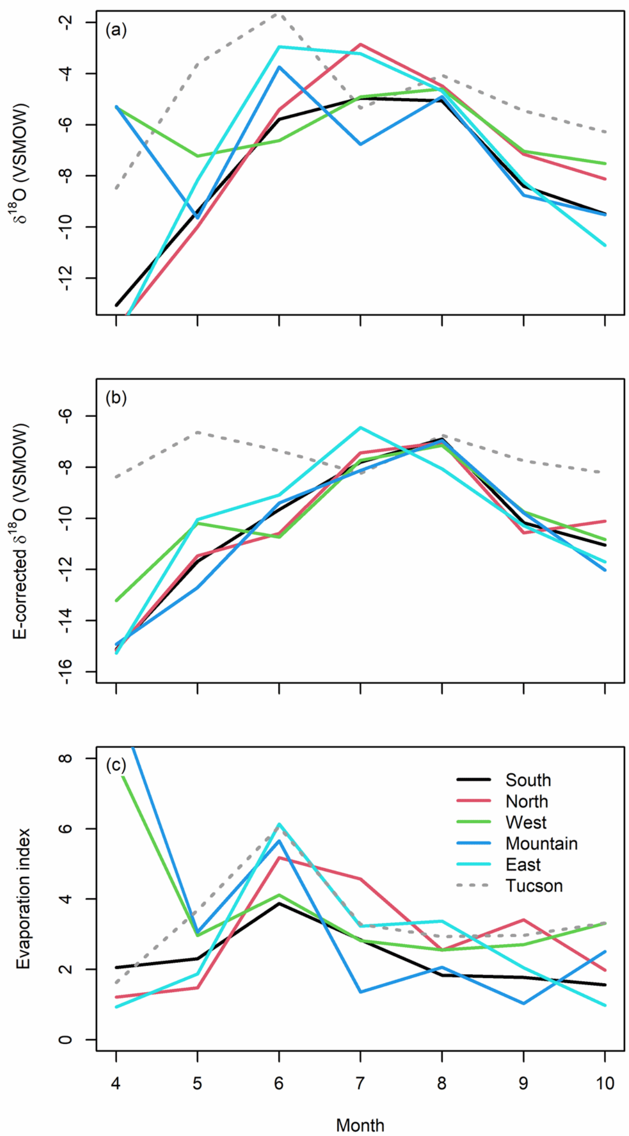

Figure 5: Monthly average precipitation isotope values for monitoring sites within each of five groups having contrasting seasonal precipitation patters (defined by Tulley−Cordova et al., 2018) and at Tucson, AZ (Eastoe & Dettman, 2016). A) Measured oxygen isotope values. B) Oxygen isotope values after correction of evaporation effects using the iSW_E method (see Methods; Bowen et al., 2018). C) The iSW_E oxygen isotope evaporation index (higher index value indicates a larger amount of post-condensation evaporation).

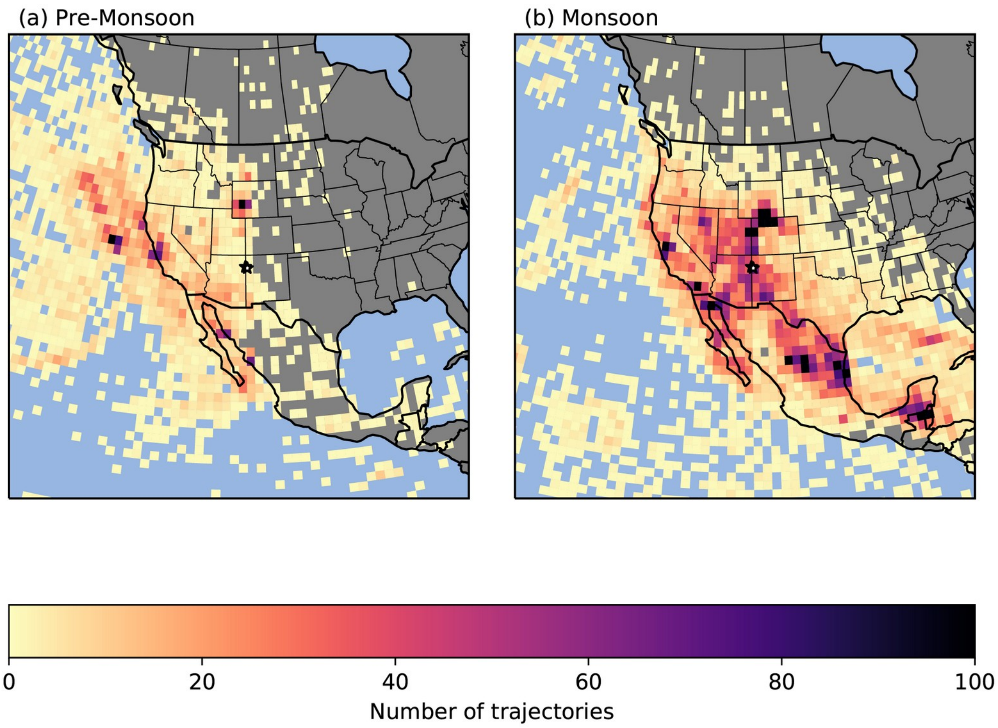

Figure 6. Spatial distribution of the vapor source region by season for combined precipitation events at Rock Springs, NM and Fort Defiance, AZ, with the representative location indicated by star. This figure shows the number of trajectories traced to a vapor source in a particular pixel during the premonsoon season (a) and monsoon season (b).

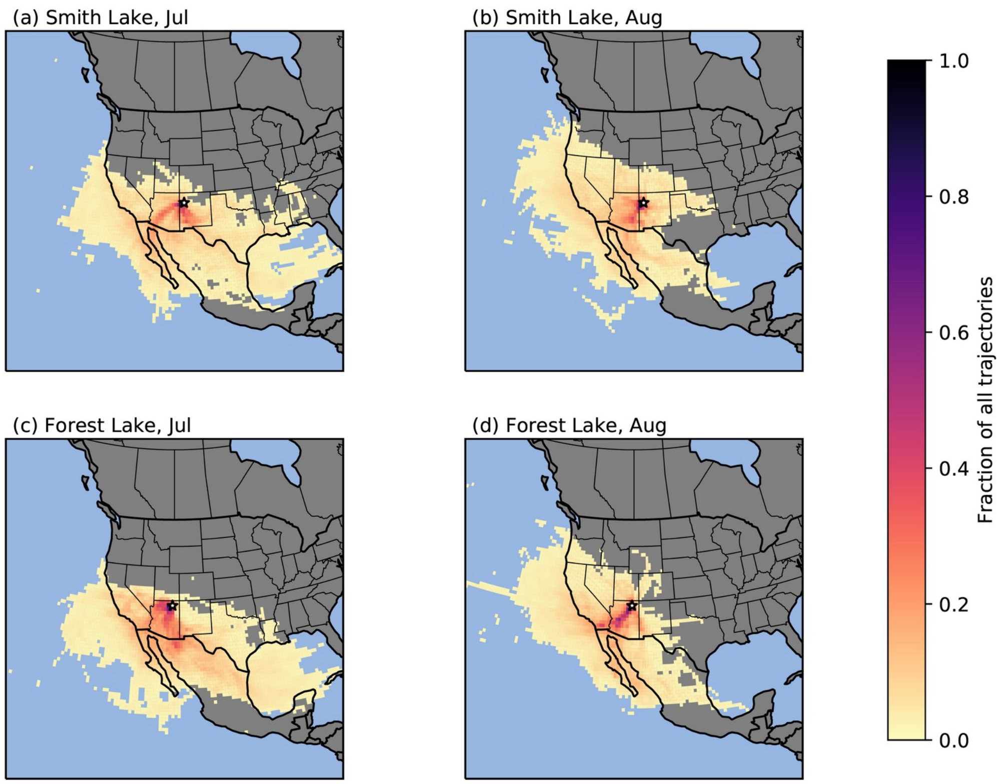

Figure 7. Spatial and temporal evolution of air mass trajectories into the Eastern (Smith Lake, NM, panels a and b) and Western (Forest Lake, AZ, panels c and d) regions of the Navajo Nation as monsoon season develops between the months of July (panels a and c) and August (panels b and d), 2016.

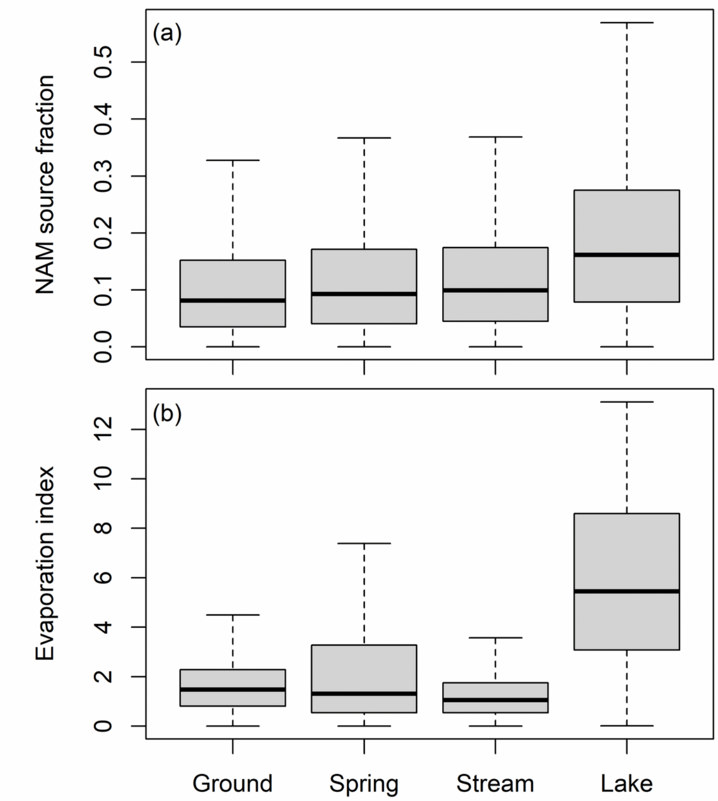

Figure 8: Posterior parameter distributions for water resource mixing model analyses. A) Estimated fractional contribution of NAM rainfall to sampled water resources. B) Oxygen isotope evaporation index distributions for each resource type. Outlier values are omitted.